Reversed Drifting Quasi-periodic Pulsating Structure in an X1.3 Solar Flare on 2005 July 30

Rui Wang, Baolin Tan, Chengming Tan and Yihua Yan
Key Laboratory of Solar Activity, National Astronomical Observatories, Chinese Academy of Sciences, Beijing, 100012, China.
Email: Ray@nao.cas.cn

Received: ****; Accepted: 7 January 2012

Abstract.

Based on the analysis of the microwave observations at frequency of 2.60 – 3.80 GHz in a solar X1.3 flare event observed at *Solar Broadband RadioSpectrometer* in Huairou (SBRS/Huairou) on 2005 July 30, an interesting reversed drifting quasi-periodic pulsating structure (R-DPS) is confirmed. The R-DPS is mainly composed of two drifting pulsating components: one is a relatively slow very short-period pulsation (VSP) with period of about 130 – 170 ms, the other is a relatively fast VSP with period of about 70 – 80 ms. The R-DPS has a weak left-handed circular polarization. Based on the synthetic investigations of *Reuven Ramaty High Energy Solar Spectroscopic Imaging* (RHESSI) hard X-ray, *Geostationary Operational Environmental Satellite* (GOES) soft X-ray observation, and magnetic field extrapolation, we suggest the R-DPS possibly reflects flaring dynamic processes of the emission source regions.

Keywords: Sun: quasi-periodic pulsation — Sun: microwave burst — Sun: flares

1. Introduction

Quasi-periodic pulsations (QPPs) associated with solar flares are observed frequently in optical, EUV, soft X-ray, hard X-ray, and radio emissions (see the recent review of Nakariakov and Melnikov, 2009). For pulsation events, Aschwanden (1987, 2004) presented an extensive review about the models, and classified them mainly into three groups: (1) magnetohydrodynamic (MHD) flux tube oscillations (eigenmodes); (2) Cyclic self-organizing systems of plasma instabilities; (3) Modulation of periodic electron acceleration. Based on the radio observations and the period of pulsation (P), QPPs can be classified into three types (Wang and Xie, 2000): (1) long period pulsation (LPP), P $\sim$ tens of seconds; (2) short period pulsation (SPP), P $\sim$ several seconds; and (3) very short period pulsation (VSP), P $\sim$ subseconds. Recently, some supplements and extensions had made the classification more comprehensive and detailed (Tan et al, 2010). The very long period pulsation (VLP) was added, whose period is in the hectosecond or several minutes range. Generally it is defined as P $>$ 100 s. On the other hand, the VSP was divided into two sub-classes: slow-VSP, where the period is in the decisecond, 0.1 $<$ P $<$ 1.0 s and the other is fast-VSP, P $<$ 0.1 s. The different QPPs should be corresponding to different generation mechanisms, and might reveal different physical conditions

in the source region. The flare-associated QPP can provide information of solar flaring regions, and give some prospective insight into coronal plasma dynamic processes, providing remote diagnostics of the microphysics of energy release sites. The understanding of flaring QPP in the solar corona will open up very interesting perspectives for the diagnostics of stellar coronae (Mathioudakis, et al., 2003).

Usually, some QPPs frequently have another important feature: frequency-time drift, recognized as drifting quasi-periodic pulsating structures (DPS) (Kliem, Karlický, and Benz, 2000). The analysis of the frequency drift rate in DPS may provide information not only about the dynamical processes of the source region but it can also reveal atmospheric properties. Kliem, Karlický, and Benz (2000) proposed a model in which the decimetric DPS is caused by quasi-periodic particle acceleration episodes that result from a highly dynamic regime of magnetic reconnection in an extended large-scale current sheet above the soft X-ray flare loop, where reconnection is dominated by repeated formation and subsequent coalescence of magnetic islands, known as secondary tearing modes. With this model, they explained the global frequency drifting pulsating structure as a motion of the plasmoid in the solar atmosphere with density gradient. Here, particles are accelerated near the magnetic X-points in the DC electric field associated with magnetic reconnection. The strongest electric fields occur at the main magnetic X-points adjacent to the plasmoid, and a large fraction of the accelerated particles may be temporarily trapped in the plasmoid; the accelerated process itself may form an anisotropic velocity distribution, which excites the observed radio emission. In fact, there are a series of works to explain DPSs as the radio emission being generated during multi-scale tearing and coalescence processes in the extended current sheet of a flare (Karlicky, 2004; Karlicky et al., 2005). Based on particle-in-cell simulation, Karlicky and Barta (2007) found that electrons are accelerated most efficiently around the X-point of the magnetic configuration at the end of the tearing process and the beginning of plasmoid coalescence. The most energetic electrons are mainly localized along the X-lines of the magnetic configuration.

However, so far, from the observations, we only obtained DPS with single-directional frequency drifting rate, i.e., drift from high frequency to lower frequency, or from low frequency to higher frequency in the single DPS event. A DPS with double-directional frequency drifting rate, i.e., the emission drifts from higher frequency to lower and then reversed, namely from lower frequency to higher may be called as reversed drifting quasi-periodic pulsating structure (R-DPS). By scrutinizing the microwave observation data obtained in *Chinese Solar Broadband RadioSpectrometer* (SBRS/Huairou), we find a particular example of R-DPS in the flare on 2005 July 30.

This paper is arranged as follows. Section 2 presents the observational data and the data analysis. Section 3 gives some discussions on physical processes related to the R-DPS. Finally, Section 4 draws our conclusions.

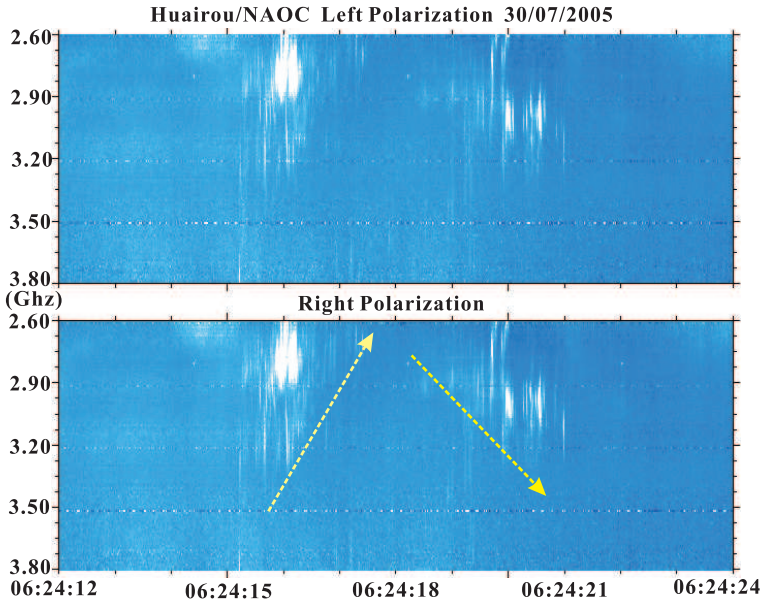

Figure 1. The spectrum of the solar microwave drifting quasi-periodic pulsating structure at 06:24:12 UT – 06:24:24 UT, on 2005 July 30, observed at SBRS/Huairou with the spectrometer of 2.60 – 3.80 GHZ. Two yellow arrows indicate frequency drifting directions.

2. Observations and Data Analysis

2.1. Observations

On 2005 July 30 an X1.3 flare/CME event occurred from 06:10 UT to 07:00 UT, with the peak at 06:35 UT in AR 10792 at N11°, E52°, near the east edge of the solar disk. During this flare event, several solar telescopes got the perfect observational data, such as the solar microwave (SBRS/Huairou), *Reuven Ramaty High Energy Solar Spectroscopic Imaging* (RHESSI) hard X-ray, *Geostationary Operational Environmental Satellite* (GOES) soft X-ray, optical *Michelson Doppler Imager* on *Solar and Heliospheric Observatory* (MDI/SOHO), and *Big Bear Solar Observatory* (BBSO), etc. In this work, our focus is on the microwave observations. We mainly use the observation of SBRS/Huairou to investigate the properties of QPP. SBRS/Huairou includes three parts: 1.10 – 2.06 GHz, 2.60 – 3.80 GHZ and 5.20 – 7.60 GHz (Fu et al., 1995; Fu et al., 2004; Yan et al., 2002). R-DPS appeared in the frequency band of 2.60 – 3.80 GHz and the time range from 06:24:15 – 06:24:21 UT, and the duration lasts for about 6 s (Figure 1).

The antenna diameter of the SBRS/Huairou at frequency of 2.60 – 3.80 GHz is 3.2 m. It is controlled by a computer to automatically trace the solar disk center and can receive the total flux of solar radio emission with dual

circular polarization. The dynamic range of this instrument is 10dB above quiet solar background emission and the observation sensitivity is $\triangle S/S_{\odot} \leq 2\%$, where $S_{\odot}$ is the quiet solar background emission. The data processing used the software in IDL language and data calibration followed the method proposed by Tanaka et al. (1973). The standard flux values of the quiet Sun are adopted from the data published by the Solar Geophysical Data (SGD). For strong bursts, the receiver may work beyond its linear range and a nonlinear calibration method will be used instead (Yan et al., 2002).

In order to make our data more convincible, the other instruments were also utilized to support the radio emission data. The soft X-ray data from GOES was used to make a comparison. Also hard X-ray observations with different energy ranges from RHESSI were adopted. In addition, the photospheric magnetograph of the line-of-sight magnetic component obtained from MDI/SOHO was adopted to extrapolate and model the coronal magnetic field.

2.2. Data Analysis

Figure 1 presents the QPP event, which occurred at 06:24:15 – 06:24:21 UT, on 2005 July 30 in the frequency range of 2.60 – 3.50 GHz. The upper and lower panels give the left- and right-handed circular polarization, respectively. From this figure, we can see that the QPP had a negative frequency drift rate (drift from high frequency to the lower frequency) during 06:24:15 – 06:24:18 UT (named left wing, hereafter), and then the frequency drift rate became positive (drift from low frequency to the higher frequency) during 06:24:18 – 06:24:21 UT (right wing), with the inflexion occurring around 06:24:18 UT. The two yellow arrows indicate the frequency drifting directions. With a linear fit we find that the frequency drift rates at each wing of the QPP are -285 MHz s^{-1} and 186 MHz s^{-1}, respectively.

In order to make sure that the QPP signals originate from the flare bursts and they are not simply noise, Figure 2 presents three profiles at the frequencies of 2.80, 3.00, and 3.20 GHz, respectively. From the SGD database we may extrapolate that the radio mean flux at frequency 2.60 – 3.80 GHz of the quiet Sun on 2005 July 30 is about 100 – 135 sfu. So the instrument sensitivity is about $\triangle S/S_{\odot} \leq 2\% \simeq 2 - 2.7$ sfu. Figure 2 indicates that there are enhancements of more than 15 sfu in the left and right wings of the QPP with respect to the background emission. Moreover the enhancements around the QPP exceed the instrument sensitivity greatly, so we may confirm that the QPP is real, this dynamic spectrum is clear and reliable.

Figure 1 shows that the patterns or intensities of the QPP are almost the same in the left-handed or right-handed polarization spectrogram, indicating that the polarization of the QPP is not obvious. Calculation indicates that the total polarization degree ($(R-L)/(R+L)$) is around -0.04%, the polarization degree of left wing is around -2.33% and the right wing is around -3.22%, where

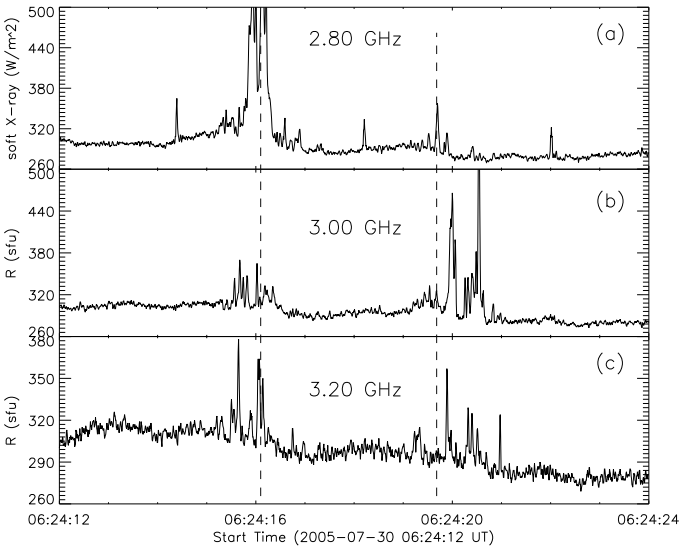

Figure 2. The profiles of radio emission at frequencies 2.80 GHz, 3.00 GHz and 3.20 GHz, respectively. The dashed lines mark the positions of the maximum flux intensity at 2.80 GHz. The relative positions to the dashed lines of the maximum flux intensity at 3.00 GHz and 3.20 GHz reflect the frequency drift rates at the left and right part of the R-DPS.

R and L are the intensities of the right- and left- handed circular polarization emission which subtract the background components, respectively.

From the bright lines of the left and right wings of the structure in Figure 1, we find that it is quasi-periodic, maybe it is hybrid of more periodic components than one. The best way to analyze this kind of structures is by using wavelet analysis, which can get information on both the amplitude of any periodic component within the series, and the temporal evolution of the QPP.

Figure 3 presents the wavelet spectrum at frequency of 3.00 GHz during 06:24:14 UT to 06:24:22 UT which just contains the time interval of the QPP. The black contours plot the confident region with 95% confidence level. In the left part of the figure, there are two obvious spectrum peaks corresponding to the left wing of the QPP in the confident region, the periods are about 80 ms (marked as A1) and 170 ms (marked as B1), respectively. This implies that there are two pulsating components overlapped around 06:24:16 UT. On the right wing, the analogous structures appear between 06:24:20 UT and 06:24:21 UT and the periods are about 70 ms (marked as A2) and 130 ms (marked as B2), respectively, which are slightly shorter than that in the left wing. Both of them are VSPs.

According to the analysis above, we could find some significant relations between the left wing and right wings of this QPP. Firstly, the gap between

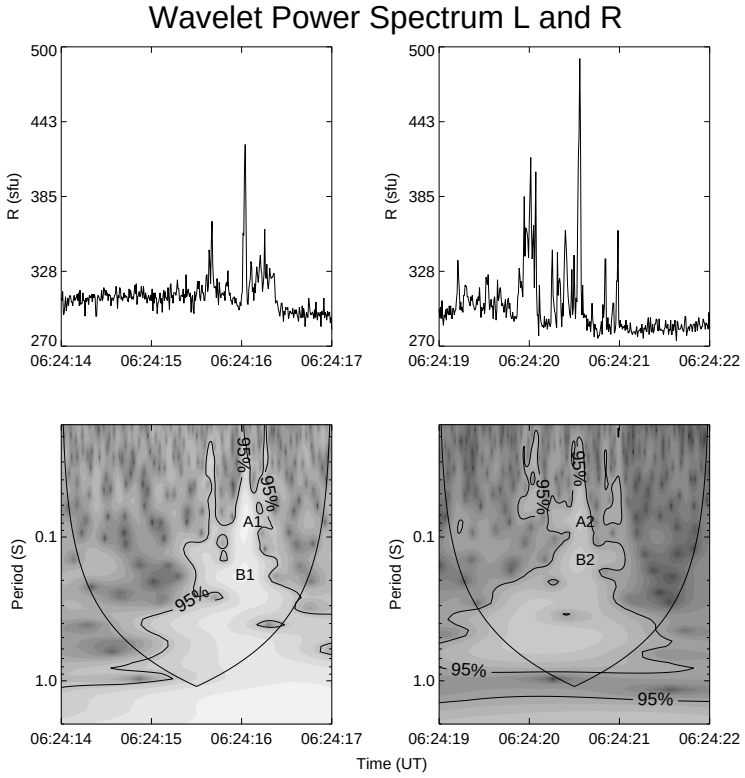

Figure 3. The bottom two panels show the wavelet power spectrum at the left and right part of R-DPS, using the Morlet wavelet. The black contours are the 95% confidence regions and anything "below" this line is dubious. The region below the parabolic curve indicates the "cone of influence", where edges influence is important. The A1 $\sim$ 80 ms, B1 $\sim$ 170 ms, A2 $\sim$ 70 ms, B2 $\sim$ 130 ms. The top two panels give corresponding radio fluxes for time comparison.

the two parts is only about 1 second, which is much shorter than the duration of each part in the QPP; secondly, the periods are very close in each part (80 ms at A1 to 70 ms at A2, 170 ms at B1 to 130 ms at B2, respectively) of the emission frequency band; thirdly, both of the degrees of polarization at each part of the QPP are not obvious. Therefore, the name R-DPS should be more appropriate to describe such kind of structures.

Figure 4 presents context data to the microwave at 2.80 GHz (which has a similar overall profile with that in the other frequencies), GOES soft X-rays, and RHESSI hard X-rays associated with the X1.3 flare/CME event from 06:10 UT to 07:00 UT. Here, the R-DPS is marked with a black arrow, which indicates that the R-DPS occurred in the flare ascending phase, just after the onset of the flare. It is associated with a time just when the gradient of the soft X-ray reaches to its maximum. RHESSI also observed this flare event,

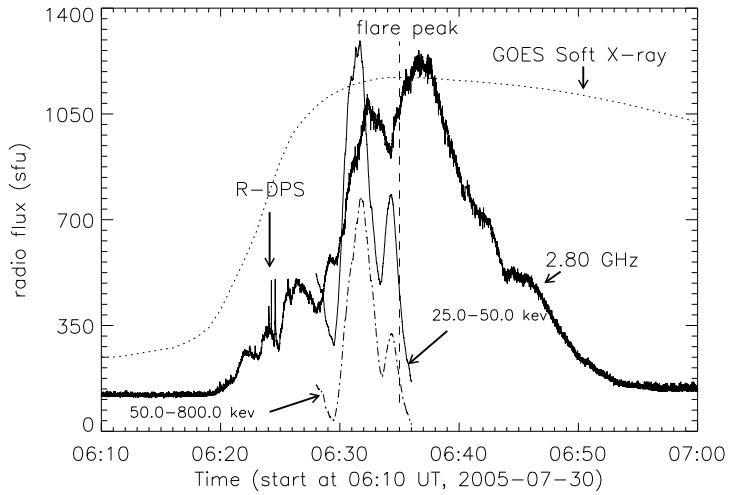

Figure 4. The relative position of the reversed drifting quasi-periodic pulsation (R-DPS) in the profile of the X1.3 flare event on July 30, 2005. The thick curve presents the profile of solar radio emission observed at frequency 2.80 GHz with SBRS/Huairou spectrometer. The thin curve and dot-dashed curve are the RHESSI hard X-ray curves in 25.0 – 50.0 kev and 50.0 – 800.0 kev, respectively. The dotted line shows soft X-rays from GOES satellite. The flare peak of this radio emission occurred at 06:35 UT.

however, we have obtained RHESSI hard X-ray data only in the time interval from 06:28 UT to 06:36 UT, and no valid data during the R-DPS. Anyway, we still present the hard X-ray emission curves in 25 – 50 keV and 50 – 800 keV as reference.

The magnetic field configuration has importance for understanding the physical processes of the QPP. Figure 5 gives the magnetic topology of the flare active region AR 10792 obtained from potential extrapolation computed from the observed line-of-sight magnetic field using a Green's function. The initial version of this technique is implemented by T. Metcalf and G. Barnes on 2005 October 25 and this program can be found in the SolarSoftWare (SSW). The background of the magnetic extrapolation in the bottom panel is the line-of-sight magnetogram observed by MDI/SOHO. Red lines present closed magnetic field lines, while blue lines are open field lines. Through the magnetic model, we can make rough scale estimations of the coronal loops. However, as there is no microwave imaging observation at the corresponding frequency, we do not know which loop is associated with the R-DPS exactly. For comparison, we present the Hα image in the same area (the upper panel in Figure 5). By reason of lacking data in the same time range, here we just got a image of AR 10792 at 06:35:49 UT on 2005 July 30, observed by BBSO, while

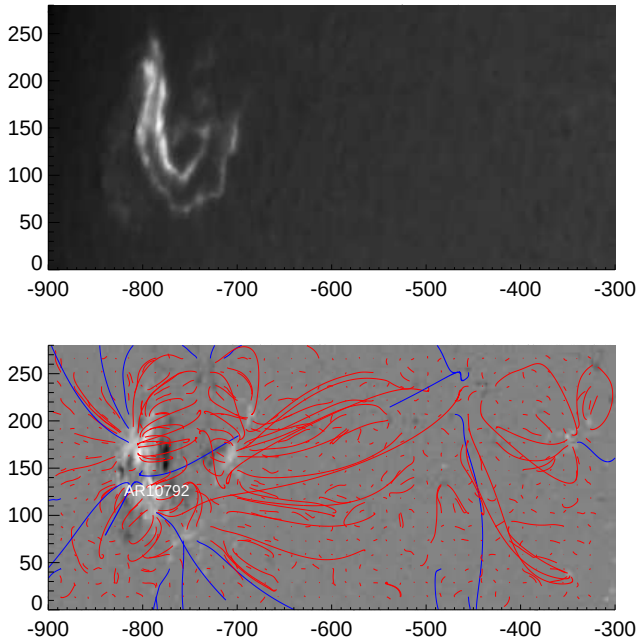

Figure 5. Potential extrapolation of magnetic field lines in the lower panel using the observed line-of-sight field of the MDI/SOHO during 06:24:12 – 06:24:24 UT, on July 30, 2005. Coordinates are in arcseconds. The coordinate of the center of the Sun is (0,0). The image in the upper panel is from the Hα data of the Big Bear Solar Observatory (BBSO) at 06:35:49 UT. There is an obvious two-ribbon flare in this image.

it is still valuable for comparison with the extrapolated model. It is obvious that there is a two-ribbon flare in this image. This structure often indicates that magnetic reconnection has allowed the coronal magnetic field to relax into a lower energy state. Practically, it is natural to assume that only the coronal loops which are adjacent to the flare ribbons are related to the microwave bursts. From Figure 5 we may obtain the lengths of these coronal loops are about 2" – 100". Suppose the coronal loops are semicircles, then the lengths of the coronal loops are about 2.3×10^3 – 1.14×10^5 km.

3. Discussion on the possible process of R-DPS

According to the work of Tan et al. (2007), Tan (2008) and Tan et al. (2010), VSP can be explained as a result of modulations of the resistive tearing-mode

oscillation in some electric current-carrying flare loops. The pulsating emission is possibly plasma emission. As we know that the plasma emission is always generated at the plasma fundamental frequency (ω_{pe}) or at the second harmonic frequency ($\sim 2\omega_{pe}$). The degree of polarization of fundamental plasma emission is very strong and usually in the sense of O-mode, while the second harmonic plasma emission is always a weak circular polarization. As the R-DPS is weakly polarized, we may suppose that it is possibly related to the second harmonic plasma emission. The central frequency of the R-DPS is about 3.00 GHz, and implies that the plasma density is about $2.78\times10^{10}\mathrm{cm}^{-3}$. Plasma with such high density is probably very close to the flare core.

Based on the plasma emission mechanism, we have the emission frequency: $f = sf_{pe} \simeq 9sn_e^{1/2}$, we may obtain the frequency drift rate as:

$$\frac{df}{dt} \simeq \frac{f}{2H}v \tag{1}$$

Here, $H = \mid n_e/\frac{dn_e}{dr} \mid$ is the inhomogeneous scale length of the plasma in the source, $v = \frac{dr}{dt}$ is the moving velocity of the emission source region. Then we may get the moving velocity: $v = \frac{2H}{f}\frac{df}{dt} = 2H\varepsilon$, $\varepsilon = \frac{1}{f}\frac{df}{dt}$ is the relative frequency drift rate. From here we know that the moving velocity is only proportional to the relative frequency drift rate. Usually, the inhomogeneous scale length H should be induced from the solar active region atmospheric model. For simplicity, we may assume that $H \sim 10^4$ km. Then we may estimate that the source moving velocity associated with the left wing of the R-DPS is about 1900 km s^{-1} , and 1240 km s^{-1} in opposite direction with the right wing. This may imply that the R-DPS reflects a following process: during the rising phase of the X1.3 flare, the closed flaring coronal loop has an upthrust in velocity of 1900 km s^{-1}, and then falls down slowly in velocity of 1240 km s^{-1}.

To the explanation of the loop upward and downward movings, a two-dimensional (2D) resistive-MHD numerical simulation of the reconnection starting from the Harris-type current sheet has been done (Bárta, Všnak, and Karlický, 2008). The result of simulation indicated that if the reconnection rate v×B at the X-point below the plasmoid is higher than the one at the X-point above the plasmoid, the plasmoid moves upward since the net tension causes an upward electron acceleration and then excites the plasma emission in the upper source region. If the magnetic flux is reconnected in the upper diffusion region is higher than in the lower one, the plasmoid moves downward and the high energy electron flow excites plasma emission from the lower source region. However as it is stated above, if the source regions are located at different altitudes, the density of the source regions would be very different, depending on the altitudes, and then different waveband signals from the right and left wing of the R-DPS would be received. This does not agree with our

observation, that the frequency range of the R-DPS event from 2.60 GHz to 3.80 GHz. Therefore we take another way to interpret our observations.

If the emission source region could be located within a loop with up-and-down motions, it would be more consistent with the observation. We assume that the up and down motions corresponded to the expansion and shrinkage of the loops. These processes should have a relation with intense energy injection (Li and Gan, 2005). During the shrinkage of the loops, there were few intense energy injections, since the chromospheric evaporation needed several minutes to fill the loops, and during this time the density of loops was rather low while it was opposite around the loops. Afterward, the injection process completed, the density of the region above the loop top was lower corresponding to the loop system, then the loop began to expand.

We may assume that the flaring loop is current-carrying plasma loop, having an up-and-down motion, a resistive tearing-mode instability will be triggered in the flaring loop and a series of multi-scale magnetic islands would form. Electron acceleration will occur at X-points between every two adjacent magnetic islands. Then the energetic electrons will excite some Langmuir turbulence in the flare plasma loop and make the plasma emission enhanced. Modulated by the resistive tearing-mode oscillation, the emission will behave as pulsating structure in the spectrogram.

At the same time, we know there are two pulsating components in both the left and right wings of the R-DPS, and this may indicate that there are two different flaring plasma loops in the same oscillating source region. The difference may be in loop radius, or electric current, etc. (Tan, 2008). However, as we have no corresponding imaging observations, we could not confirm which factor is the real candidate.

4. Conclusions

In this work we present detailed observations of a particular reversed drifting quasi-periodic pulsation (R-DPS) associated with the rising phase of an X1.3 flare event. From the above data analysis and discussions, we may reach the following conclusions:

(1) It is observationally confirmed that the theoretically predicted reversed direction frequency drift structures in microwave emission indeed exist.

(2) The R-DPS is mainly composed of two pulsating components: one is a slow-VSP with period of about 130 – 170 ms, the other is a fast-VSP with period of about 70 – 80 ms.

(3) The frequency drift rate in the left wing of the R-DPS is about -285 MHz s^{-1}, and in the right wing about 186 MHz s^{-1}.

(4) The polarization of the R-DPS is a weak left-handed circular polarization.

Based on the assumption of plasma emission mechanism that the tearing mode oscillation modulates the plasma emission in current-carrying plasma loops, the R-DPS may reflect the dynamic processes of the emission source regions. From the frequency drift rates we make an estimation of the source up-and-down motion velocity being about 1900 km s^{-1} up and then 1240 km s^{-1} down. The variations of the plasma density in the loop with respect to the background during the up-and-down motion result the reversed drifting quasi-periodic pulsations. In order to confirm this deduction, some microwave imaging observations at the corresponding frequency is necessary. The constructing *Chinese Spectral Radioheliograph* (0.4 – 15 GHz) will satisfy this need (Yan et al, 2009).

Acknowledgements

The authors would like to thank the referee for the helpful and valuable comments on this paper. We would also thank the the GOES, RHESSI, MDI/SOHO, BBSO and SBRS/Huairou teams for providing observation data. This work was supported by NSFC Grant No. 10873021, 10921303, 10903013, 11103044, 11103039, MOST Grant No. 2011CB811401, and the National Major Scientific Equipment R&D Project ZDYZ2009-3.

References

Aschwanden, M.J.: 1987, *Solar Phys.* **111**, 113.
Aschwanden, M.J.: 2004, *Physics of the Solar Corona: An introduction, Springer, Berlin.*
Bárta, M., Vršnak, B., Karlický, M.: 2008, *Astron. Astrophys.* **477**, 649.
Fu, Q.J., Qin, Z.H., Ji, H.R., Pei, L.B.: 1995, *Solar Phys.* **160**, 97.
Fu, Q.J., Ji, H.R., Qin, Z.H., Xu, J.C., Xia, Z.G., Wu, H.A., Liu, Y.Y., Yan, Y.H., Huang, G.L., Chen, Z.J., Jin, Z.Y., Yao, Q.J., Cheng, C.L., Xu, F.Y., Wang, M., Pei, L.B., Chen, S.H., Yang, G., Tan, C.M., Shi, S.B.: 2004, *Solar Phys.* **222**, 167.
Li, Y.P., Gan, W.Q.: 2005, *Astrophys. J.* **629**, 137.
Karlický, M.: 2004, *Astron. Astrophys.* **417**, 325.
Karlický, M., Bárta, M.: 2007, *Astron. Astrophys.* **464**, 735.
Karlický, M., Bárta, M., Mészárosová, H., Zlobec, P.: 2005, *Astron. Astrophys.* **432**, 705.
Kliem, B., Karlický, M., Benz, A.O.: 2000, *Astron. Astrophys.* **360**, 715.
Mathioudakis, M. Seiradakis, J.H., Williams, D.R., Avgoloupis, S., Bloomfield, D.S., McAteer, R.T.J.: 2003, *Astron. Astrophys.* **403**, 1101.
Nakariakov, V.M., Melnikov, V.F.: 2009, *Space Sci. Rev.* **149**, 119.
Tan, B.L.: 2008, *Solar Phys.* **253**, 117.
Tan, B.L., Yan, Y.H., Tan, C.M., Liu, Y.Y.: 2007, *Astrophys. J.* **671**, 964.
Tan, B.L., Zhang, Y., Tan, C.M., Liu, Y.Y.: 2010, *Astrophys. J.* **723**, 25.
Tanaka, H., Castelli, J.P., Covington, A.E., Krüger, A., Landecker, T.L., Tlamcha, A.: 1973, *Solar Phys.* **29**, 243.
Wang, M., Xie, R.X.: 2000, *China. J. Astron. Astrophys.* **24**, 95.

Yan, Y.H., Tan, C.M., Xu, L., Ji, H.R., Fu, Q.J., Song, G.X.: 2002, *Science in China Ser. A* **45**, 89.
Yan, Y.H., Zhang, J., Wang, W., Liu, F., Chen, Z.J., Ji, G.S: 2009, *Earth Moon Planet* **104**, 97.